

1 **Use of stable isotope probing to assess the fate of emerging**
2 **contaminants degraded by white-rot fungus**

3
4 Marina Badia-Fabregat¹, Mònica Rosell², Glòria Caminal³, Teresa Vicent¹,
5 Ernest Marco-Urrea^{1,*}

6
7 ¹Departament d'Enginyeria Química, Escola d'Enginyeria, Universitat Autònoma de
8 Barcelona, 08193 Bellaterra, Barcelona (Spain)

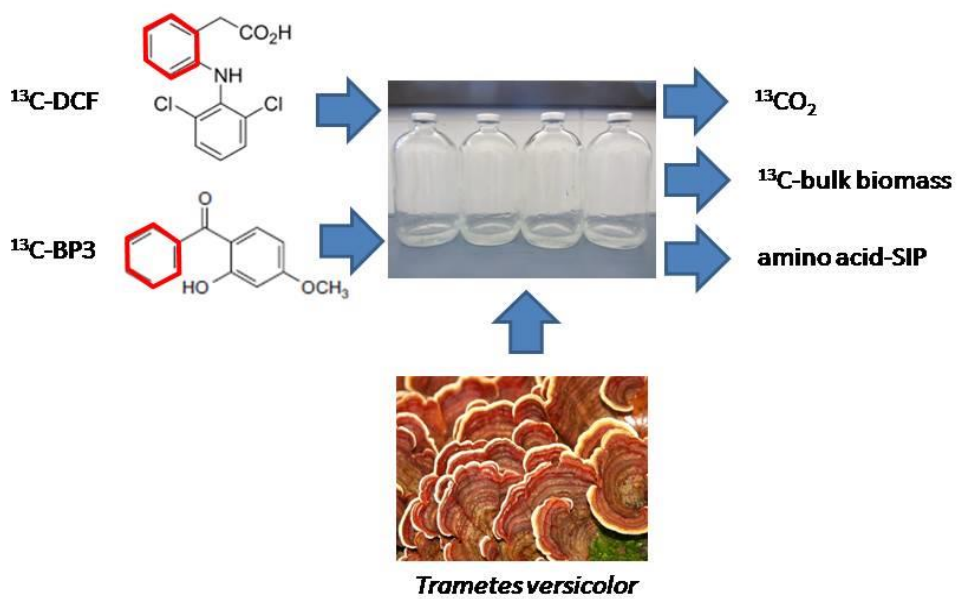
9 ²Grup de Mineralogia Aplicada i Medi Ambient, Departament de Cristal·lografia,
10 Mineralogia i Dipòsits Minerals, Facultat de Geologia, Universitat de Barcelona. Martí
11 Franquès s/n, 08028 Barcelona (Spain)

12 ³Institut de Química Avançada de Catalunya. IQAC-CSIC. Jordi Girona 18-26. 08034
13 Barcelona (Spain)

14
15 * Corresponding author: Departament d'Enginyeria Química, Escola d'Enginyeria,
16 Universitat Autònoma de Barcelona, 08193 Bellaterra, Barcelona (Spain). Tel: +34-
17 5868372. E-mail: Ernest.Marco@uab.cat.

18

19 Graphical abstract/TOC



20
21

22

23 **Abstract**

24 The widespread of emerging contaminants in the environment and their potential
25 impact on humans is a matter of concern. White-rot fungi are cosmopolitan organisms
26 able to remove a wide range of pharmaceuticals and personal care products (PPCP)
27 through cometabolism (i.e. laccases and peroxidases) or detoxification mechanisms
28 (i.e. cytochrome P450 system). However, the use of PPCP as carbon source for these
29 organisms is largely unexplored. Here, we used carbon stable isotope tracer
30 experiments to assess the fate of anti-inflammatory diclofenac (DCF) and UV filter
31 benzophenone-3 (BP3) during degradation by *Trametes versicolor*. The comparison
32 between carbon isotopic composition of emitted carbon dioxide from ^{13}C -labelled DCF
33 ([acetophenyl ring- $^{13}\text{C}_6$]-DCF) and ^{13}C -BP3 ([phenyl- $^{13}\text{C}_6$]-BP3) versus their ^{12}C -
34 homologue compounds showed mineralization of about 45% and 10% of the ^{13}C
35 contained in their respective molecules after 9 days of incubation. The carbon isotopic
36 composition of the bulk biomass and the application of amino acid-stable isotope
37 probing (SIP) allowed distinguishing between incorporation of ^{13}C from BP3 into amino
38 acids, which implies the use of this emerging contaminant as carbon source, and major
39 intracellular accumulation of ^{13}C from DCF without implying the transformation of its
40 labelled phenyl ring into anabolic products. A mass balance of ^{13}C in different
41 compartments over time provided a comprehensive picture of the fate of DCF and BP3
42 across their different transformation processes. This is the first report assessing
43 biodegradation of PPCP by SIP techniques and the use of emerging contaminants as
44 carbon source for amino acid biosynthesis.

45

46 **Keywords**

47 Fungi, Stable Isotope Probing (SIP), Diclofenac, Benzophenone-3, Mineralization,
48 Amino acids.

49

50 **1. Introduction**

51 The presence of emerging contaminants in the environment raises concerns about its
52 potential to harm human or environmental health (Brausch and Rand, 2011; Murray et
53 al., 2010). The anti-inflammatory diclofenac (DCF) and the UV filter benzophenone-3
54 (BP3) have high levels of consumption, widespread presence in the environment (Duan
55 et al., 2013; Fent et al., 2010; Liu et al., 2011; Barbara Morasch, 2013) and significant
56 associated environmental risk (Hernando et al., 2006). DCF was recently proposed to
57 be included as priority substance in the Water Framework Directive 2000/60/EC
58 (European Commission, 2012). Regarding BP3, it is regulated by the 2002/72/EC
59 Directive, relating to compounds in contact with food, and was listed as substance with
60 potential evidence of endocrine disrupting effects (category 2) (European Commission,
61 2007).

62 In order to avoid the release of xenobiotics, some alternative strategies are under study
63 as conventional wastewater treatment plants (WWTP) are not effective in totally
64 degrading these compounds (Jelic et al., 2011). The use of ligninolytic fungi is one of
65 these alternatives and their application as decontaminating agent has been intensively
66 studied during the last years (Golan-Rozen et al., 2011; Harms et al., 2011). Both DCF
67 and BP3, together with many other PPCP, were previously shown to be biodegradable
68 by white-rot fungi (Gago-Ferrero et al., 2012; Marco-Urrea et al., 2010; Marco-Urrea et
69 al., 2009). However the mechanistic of PPCP degradation is still not fully understood
70 and has stated to proceed either cometabolically by means of extracellular enzymes
71 such as laccases and peroxidases or via detoxification reactions such as cytochrom
72 P450 and conjugations (Yang et al., 2013). For bioremediation purposes, metabolic or
73 growth-linked reactions are preferred over cometabolic or detoxification mechanisms
74 since microorganisms can derive their carbon and energy directly from the pollutant.
75 However, evidence of the use of xenobiotics as a carbon source is limited in white-rot
76 fungi.

77 To accomplish the aim of identifying biodegradation strategies that entail
78 mineralization, the use of contaminants labelled with stable carbon isotopes and further
79 determination of carbon isotopic signatures of CO₂ has been widely applied. With the
80 advent of stable-isotope probing (SIP) analyses, the range of applications increased
81 including tracking the carbon flow through microbial communities (Bastida et al., 2010)
82 and identifying unannotated pathways in certain microorganisms (Marco-Urrea et al.,
83 2012), among others. The basis of this technique is labelling certain type of microbial
84 biomarkers with stable isotopes (usually ¹³C) and then, using chromatography coupled
85 to mass spectrometry (MS) or to isotope ratio mass spectrometry (IRMS) for higher
86 sensibility, determine the increase in the ¹³C atom percentage (at%) of the labelled
87 biomarker pools. Thus, protein-SIP (Bastida et al., 2010), total lipid fatty acids (TLFA)-
88 SIP (Bastida et al., 2011; Jakobs-Schönwandt et al., 2010), DNA-SIP (Lu and
89 Chandran, 2010) or RNA-SIP (Bastida et al., 2011) analyses can be performed.

90 The application of isotope techniques to fungi can shed light on the role of these
91 widespread organisms in decontamination processes and also predict contaminant fate
92 in the environment (Harms et al., 2011). The use of SIP-techniques in fungi is scarce
93 and limited to a recent study demonstrating the incorporation of the carbon-based
94 nanomaterial C₆₀ fullerol into the lipid biomass of two white-rot fungi (*Trametes*
95 *versicolor* and *Phlebia tremellosa*) (Schreiner et al., 2009).

96 In the present study, we combine the analysis of carbon isotopic composition of CO₂,
97 bulk biomass and individual amino acids (by amino acid stable isotope probing [aa-
98 SIP]) during the degradation of ¹³C-DCF and ¹³C-BP3 by the white-rot fungus *T.*
99 *versicolor* to track the ¹³C fate of these emerging contaminants and the degradation
100 mechanism used by the fungus. This is the first work to demonstrate assimilation of
101 xenobiotics into fungal amino acids using SIP techniques.

102

103 **2. Materials and methods**

104 **2.1. Reagents and fungal strains**

105 The nonlabelled BP3 (^{12}C -BP3) was kindly provided by Merck (Darmstadt, Germany).
106 [Phenyl- $^{13}\text{C}_6$]-oxybenzone (^{13}C -BP3) was obtained from Cambridge isotopes
107 (Cambridge, UK) with a chemical purity > 99% and an isotope purity 99 at%. The
108 nonlabelled DCF (^{12}C -DCF) was purchased from Sigma-Aldrich (Saint Louis, USA).
109 [Acetophenylring- $^{13}\text{C}_6$]-diclofenac (^{13}C -DCF) was obtained from Alsachim (Strasbourg,
110 France) with a chemical purity > 99% and an isotope purity 99 at%. All other chemicals
111 used were of analytical grade.

112 *T. versicolor* (ATCC#42530) was obtained from the American Type Culture Collection
113 and was maintained by subculturing on petri dishes in malt extract (2%) and agar
114 (1.5%) medium at 25°C.

115

116 **2.2. Media and cultures for fungal production**

117 Pellets production was done as previously described by Font et al. (2003) The blended
118 mycelia suspension used for the experiments was obtained by grinding the pellets in
119 8% NaCl solution with a X10/20 homogenizer (Ystral GmbH, Dottingen, Germany). For
120 the experiments, a defined medium was used (Blázquez et al., 2004), with a glucose
121 initial concentration of 0.5 gL⁻¹ and 2 gL⁻¹ of KH₂PO₄ instead of dimethyl succinic acid to
122 minimize other possible carbon sources than glucose and contaminant.

123

124 **2.3. Experimental design**

125 Each experiment included, apart from the experimental bottles, uninoculated and
126 sodium azide killed controls for abiotic degradation and biotic sorption determination
127 respectively. DCF experiment also included heat killed controls. All experiments were

128 conducted in duplicate in 125-mL serum bottles (Wheaton, Mealville, NJ). Cultures
129 were incubated at 25°C and 130 rpm orbital agitation.

130 ¹²C- or ¹³C-BP3/DCF were added from 100 mg/L stock solution in acetonitrile (BP3) or
131 ethanol (DCF) to a final concentration of 1 mg/L, in a total volume of 10 mL of medium.
132 Acetonitrile and ethanol were totally evaporated with nitrogen before the addition of
133 medium in order to avoid their possible use as carbon source by the fungus. Finally,
134 one millilitre of blended mycelia was added to obtain a concentration of 0.5 g d.w. L⁻¹ in
135 the bottles. In the sodium azide killed controls, 100 µL of sodium azide at 100 g L⁻¹
136 were additionally added the day before and left shaking overnight with the media and
137 the fungus to ensure the total inactivation of the fungus prior to pollutant addition. Heat
138 killed controls were previously autoclaved 30 min at 121°C. The existing air inside the
139 bottles was replaced by a higher oxygen content air by means of displacing the air with
140 pure oxygen in order to avoid a potential oxygen limitation as *T. versicolor* is an aerobic
141 organism (Marco-Urrea et al., 2008). Bottles were then closed with Teflon-coated butyl-
142 stoppers (Wheaton, Millville, NJ) and aluminium crimps (Baxter Scientific Products,
143 McGaw Park, IL).

144 At each sampling point (initially, at 3, 6 and 9 days), the procedure was the same: for
145 the non sacrificed bottles at that time, the air was replaced by blowing pure oxygen
146 inside again and, for the sacrificed bottles, the procedure performed was as follows.
147 CO₂ was sampled with a gas-tight syringe from the headspace of the bottle and directly
148 injected to a gas chromatograph coupled to an isotope ratio mass spectrometer
149 through a combustion interface (GC-C-IRMS). Then, for BP3 experiment, the bottles
150 were opened and 1 mL was sampled and filtered through 0.22 µm PVDF syringe filter
151 (Millipore, US) for glucose and laccase activity analyses. Afterwards, BP3 was
152 solubilised by adding 6 mL of ethanol and the mixture was centrifuged for 10 min at
153 4°C and 13000 g. In the case of DCF, ethanol addition was not needed due to its
154 higher solubility in water. The supernatant was filtered by 0.45 µm nylon filter (Millipore,

155 US) (BP3) or 0.22µm PVDF syringe filter (Millipore, US) (DCF) and analysed by HPLC-
156 UV for contaminant quantification. The pellet was further processed for elemental
157 analysis of biomass and amino acid-SIP (aa-SIP) analysis as described below.

158

159 **2.4. Protein extraction, purification and amino acids derivatization**

160 Protocol used for protein extraction, purification and amino acids derivatization was
161 adapted from Bastida et al. (2011). Detailed information can be found at
162 Supplementary Material.

163

164 **2.5. Analytical methods**

165 *2.5.1. HPLC-UV analysis*

166 Filtered samples of the supernatant were placed in amber HPLC vials to avoid natural
167 photodegradation during the analysis. A Dionex 3000 Ultimate HPLC equipped with UV
168 detector and autosampler Dionex were used. The chromatographic separation was
169 achieved on a LiChrosphere RP-18 (125 mm x 4 mm, 5 µm) LC column (Merck,
170 Barcelona, Spain). The method used for BP3 analysis is extensively described in
171 Gago-Ferrero et al. (2012) and the method for DCF was modified from Marco-Urrea et
172 al. (2010), changing the isocratic mobile phase for a gradient elution. Acetonitrile
173 changes from 35% to 55% in 20 min, then, from 55% to 100% in 5 min, remaining at
174 100% during 5 minutes and decreasing rapidly to 35% where it is maintained 5 more
175 minutes.

176 *2.5.2. Stable isotope analysis and calculations*

177 Isotope ratios were reported in δ-notation (‰) relative to the Vienna Pee Dee
178 Belemnite standard (V-PDB, IAEA-Vienna). The δ¹³C value is defined as

179 $\delta^{13}\text{C}=(R_s/R_r-1)\times 1000$, where R_s and R_r are the $^{13}\text{C}/^{12}\text{C}$ ratios in the sample and V-
180 PDB standard, respectively. To convert $\delta^{13}\text{C}$ to atom% ^{13}C , the equation $\text{atom}\%$
181 $^{13}\text{C}=100/(1/((\delta/1000+1)R_{\text{PDB}})+1)$ was used, where δ is the measured $\delta^{13}\text{C}$ (‰) of the
182 sample and R_{PDB} is the isotope ratio of V-PDB ($R_{\text{PDB}}=0.0112372$).

183 *2.5.2.1. CO₂ analysis by GC-C-IRMS*

184 $^{13}\text{C}/^{12}\text{C}$ ratios of headspace CO₂ were determined by a GC–C–IRMS system consisted
185 of an Agilent 6890 gas chromatograph (Palo Alto, CA, USA) equipped with a
186 split/splitless injector, coupled to a Delta Plus isotope ratio mass spectrometer through
187 a GC-Combustion III interface (ThermoFinnigan, Bremen, Germany). Column
188 specifications and settings are explained in detail in the Supplementary Material.

189 *2.5.2.2. Bulk biomass analysis by EA-IRMS*

190 The carbon isotopic composition of the bulk freeze dried biomass was determined
191 using a Flash EA1112 elemental analyser (EA) coupled to a Delta C isotope ratio mass
192 spectrometer through a ConFlo III interface (ThermoFinnigan, Bremen, Germany). Delta
193 values ($\delta^{13}\text{C}$) of the samples were corrected using the linear regression derived from
194 three international reference materials (USGS 24, IAEA-CH-6 and IAEA-CH-7) and
195 with respect to the Vienna Pee Dee Belemnite (VPDB) standard according to Coplen et
196 al. (2006).

197 *2.5.2.3. Amino acids SIP analysis by GC-C-IRMS*

198 Carbon isotopic compositions of individual amino acids were determined with the same
199 GC–C–IRMS system described for CO₂. Column, temperature program and other
200 specifications can be found in the Supplementary Material.

201 *2.5.3. Other analyses*

202 Glucose concentration was measured with a biochemical analyser YSI 2700 SELECT
203 (Yellow Spring Instruments) in the concentration range $0-20 \pm 0.04 \text{ g L}^{-1}$. Laccase

204 activity was measured using a modified version of the method for the determination of
205 manganese peroxidase (Kaal et al., 1993) as described elsewhere (Gago-Ferrero et
206 al., 2012). Biomass amount was determined as the constant weight at 100 °C.

207

208 **3. Results and discussion**

209 **3.1. Mineralization**

210 Under the described experimental conditions, DCF was totally removed from the
211 solution within 3 d (Fig. 1A). As Figure 1B shows, also BP3 concentration decreased
212 quite fast from the liquid the first 3 d, but afterwards a plateau was reached achieving a
213 final removal of $81.2 \pm 5.6\%$. In both cases, negligible removal of DCF and BP3 was
214 observed in the inactivated controls, indicating that removal was not due to sorption.
215 Glucose was completely consumed during the first 3 days and laccase maximum
216 activity was around $20\text{-}30 \text{ U L}^{-1}$ (Fig. S1).

217 As shown in Fig. 2A, CO_2 production rate in the experimental bottles reached a peak
218 within the first 3 d of incubation, corresponding with the period of glucose consumption.
219 No significant differences in total CO_2 production were detected between samples
220 containing labelled and unlabelled compounds. The percentage of $^{13}\text{CO}_2$ released from
221 the labelled phenyl moieties of ^{13}C -DCF and ^{13}C -BP3 was calculated taking into
222 account the amount of CO_2 produced and the $\delta^{13}\text{C}$ values at each time. As shown in
223 Fig. 2B, mineralization of ^{13}C from DCF reached a final percentage of only 11% the
224 ninth day with respect to the initial ^{13}C , while 30% of ^{13}C from BP3 was already
225 detected as CO_2 on day 3 and 45% on day 9. At 6 and 9 d the increase in the labelled
226 ring mineralization was still considerable because CO_2 was much more enriched in ^{13}C
227 ($\delta^{13}\text{C}$ is higher) although the production was lower.

228 The $\delta^{13}\text{C}$ values of controls containing sodium azide plus ^{13}C -BP3 were identical to
229 those of controls containing sodium azide with ^{12}C -BP3 indicating that $^{13}\text{CO}_2$ production
230 was biotic. However, an unexpected ^{13}C isotopic enrichment of CO_2 was observed in
231 controls inactivated with sodium azide plus ^{13}C -DCF that reached $\delta^{13}\text{C}$ values up to
232 25.9 ± 2.1 at 9 d. However, the percentage of initial ^{13}C -DCF mineralized in these
233 controls was negligible when referred to the low CO_2 emitted in these microcosms. This
234 enrichment was probably produced by the oxidative action of extracellular laccase, not
235 fully deactivated by sodium azide, which was able to remove rapidly DCF from the
236 medium in previous *in vitro* experiments (Marco-urrea et al., 2010). To confirm this
237 aspect, thermically inactivated controls with ^{13}C -DCF were also included and resulted
238 in $\delta^{13}\text{C}$ values comparable to inactivated controls containing ^{12}C -DCF.

239 This is the first study reporting biological mineralization of BP3. Mineralization of other
240 xenobiotics had already been reported for *T. versicolor*: [$^{13}\text{C}_2$]-trichloroethylene (Marco-
241 Urrea et al., 2008), [U- ^{14}C]-pentachlorophenol (Tuomela et al., 1999) and 2,4',5-[U-
242 ^{14}C]-trichlorobiphenyl (Beaudette et al., 1998). However, mineralization percentages in
243 those cases were lower (11% on day 22 for TCB, 29% in 42 d for PCP). On the other
244 hand, other labelled PPCP compounds such as [$^{13}\text{C}_6$ -phenyl]-sulfamethazine and [$^{13}\text{C}_3$ -
245 propionic]-ibuprofen, did not show $^{13}\text{CO}_2$ production after being degraded by white-rot
246 fungi (García-Galán et al., 2011; Marco-Urrea et al., 2009).

247 Regarding DCF mineralization, we expected higher mineralization values since
248 degradation rate and removal of identified transformation products occurred more
249 rapidly than in the case of BP3 (Gago-Ferrero et al., 2012; Marco-urrea et al., 2010).
250 Biological mineralization of [$^{14}\text{C}_1$ -carboxyl]-DCF was previously shown (Al-Rajab et al.,
251 2010) in soils by the indigenous microbiota although it should be noted that the ^{14}C
252 labelled carbon was in the carboxyl group, probably easier to convert to CO_2 than the
253 aromatic ring carbons. In the present work, although only one aromatic ring of each

254 target compound was labelled, the fact that both aromatic rings are equally oxidized
255 leads to hypothesize that ring cleavage would occur similarly to the whole molecule.

256 Summarizing, mineralization rate and yield can not be inferred from the removal rate of
257 the parent compound and the main metabolites and experiments on CO₂ isotopic
258 signature are needed to unequivocally confirm mineralization.

259

260 **3.2. ¹³C incorporation into fungal biomass by EA-IRMS and amino acid-SIP**

261 A key aspect that remains vaguely explored on the use of fungi in bioremediation is
262 their ability to use xenobiotics as carbon source. Indeed, it is thought that bacteria can
263 outcompete fungus in contaminated sites because the latter cannot obtain energy for
264 growth from contaminants (Harms et al., 2011). The first step, thus, is to determine
265 whether *T. versicolor* can use the xenobiotics as carbon source or not. Afterwards,
266 further experiments should be done to confirm if fungi can grow on them as a sole
267 carbon source. Some experiments have already been done with white-rot fungi growing
268 on xenobiotics as sole carbon source (Prenafeta-Boldú et al., 2001), but they lacked
269 the information about incorporation of compounds in the anabolic pathways.

270 The bulk analysis of the $\delta^{13}\text{C}$ values of fungal biomass by EA-IRMS showed $\delta^{13}\text{C}$
271 enrichment in both cultures spiked with ¹³C-DCF and ¹³C-BP3 in comparison with the
272 $\delta^{13}\text{C}$ values observed in the unlabeled controls (¹²C-BP3 and ¹²C-DCF) which remained
273 constant over time. A marked shift in the $\delta^{13}\text{C}$ enrichment was observed the first 3 d of
274 incubation in cultures spiked with ¹³C-BP3 (from -21.9 ± 0.3 to -6.7 ± 2.5) and
275 afterwards remained constant. On the other hand, a continuous incorporation of ¹³C
276 into biomass was observed for cultures containing ¹³C-DCF, with a $\delta^{13}\text{C}$ increasing
277 from -6.4 ± 1.2 at time zero to $+28.4 \pm 3.9$ at 9 days. The carbon isotopic signature in
278 heat killed and sodium azide killed controls spiked with either labelled or unlabelled
279 BP3 and DCF resulted in $\delta^{13}\text{C}$ values statistically identical, indicating that ¹³C-

280 incorporation in live cultures was not due to passive uptake associated to physico
281 chemical processes such as sorption. The time-course of ^{13}C enrichment into biomass
282 is depicted in Fig. 3 as percentage of ^{13}C atom (at%).

283 Previous indirect evidences using specific inhibitors suggested a role to cytochrome
284 P450 system in the primary oxidation of DCF and BP3 (Gago-Ferrero et al., 2012;
285 Marco-urrea et al., 2010). This mechanism would imply an active uptake of
286 contaminants through the fungal cell wall and membranes and their further intracellular
287 transformation. In addition, the role of cytochrome P450 in DCF and BP3 degradation
288 by *T. versicolor* was underpinned by the previous identification of hydroxylated and
289 demethylated transformation products typically catalyzed by this intracellular enzymatic
290 system (Gago-Ferrero et al., 2012; Marco-urrea et al., 2010). On the one hand, DCF
291 was rapidly transformed to 4'-hydroxydiclofenac and 5-hydroxydiclofenac by *T.*
292 *versicolor* and these intermediates disappeared after 24 h from the medium (Marco-
293 urrea et al., 2010) (Fig. S2). Other white-rot fungi, such as *Phanerochaete*
294 *chrysosporium*, also degrade effectively DCF (Rodarte-Morales et al., 2012) and the
295 metabolites produced by *Phanerochaete sordida* are hydroxylations as well (Hata et
296 al., 2010). On the other hand, fungal BP3 byproducts are 4-hydroxybenzophenone, 2,4-
297 and 4,4'-dihydroxybenzophenone together with glucose and pentose conjugates (Fig.
298 S3). Both hydroxylated and conjugated byproducts of BP3 disappeared from the
299 medium after two weeks of incubation (Gago-Ferrero et al., 2012). Therefore, the
300 observed biomass labelling could be attributed to the intracellular presence of labelled
301 untransformed DCF and BP3 or associated byproducts without implying a final
302 incorporation into anabolic products.

303 Amino acids-SIP was used to unequivocally demonstrate the transformation of DCF
304 and/or BP3 into anabolic products. In Fig. 4, the amino acid enrichment (as atom %
305 ^{13}C) in cultures of *T. versicolor* spiked with ^{13}C -BP3 compared with controls spiked with
306 ^{12}C -BP3 are presented. Incorporation of ^{13}C was observed in all the target amino acids

307 since the third day of incubation, except for serine that did not show significant
308 enrichment (0.016 at%) until the sixth day of incubation. Fluctuations in the isotope
309 content over time were attributed to the continuous turnover of amino acids to
310 precursor intermediates that was reflected in the labelling patterns. The extent of
311 enrichment varies between amino acids. The highest ^{13}C incorporation (>0.05%) was
312 observed for alanine, glutamate and aspartate, which can be biosynthesized by
313 transamination of pyruvate and tricarboxylic acid (TCA) cycle intermediates α -
314 ketoglutarate and oxaloacetate respectively. A common degradation pathway of
315 aromatic compounds by white-rot fungi involves the ring cleavage to produce β -
316 ketoadipate and finally succinate and acetyl-CoA, essential compounds of TCA cycle
317 (Wells and Ragauskas, 2012). Therefore, an hypothetical metabolic pathway of BP3
318 would include i) the ring oxidation by the action of cytochrome P450 system (as
319 previously reported in Gago-Ferrero et al. (2012)), ii) catechol formation and ring
320 cleavage by ortho-fission generating an intradiol, and iii) anabolism precursors
321 formation via β -ketoadipate pathway (Fig. S3). However, these intermediates were not
322 detected by nuclear magnetic resonance analyses during the experiment, probably due
323 to their low concentration in the medium and rapid transformation (data not shown).
324 Interestingly, ^{13}C incorporation of amino acids are in the same range than the global
325 incorporation observed in bulk biomass (0.02 at%), except for glutamate, aspartate,
326 alanine, threonine and proline that showed higher values.

327 Regarding DCF, no significant ^{13}C incorporation was detected in the amino acids.
328 These results may suggest that DCF (or byproducts) can be accumulated into the cell
329 for being further transformed by the cytochrome P450 system, as previous inhibitory
330 experiments indicated (Marco-urrea et al., 2010) and thus contributing to the high
331 isotopic enrichment observed in the bulk biomass. Therefore, our results indicate that
332 DCF would be mineralized mainly by cometabolic pathways instead of being used as
333 carbon source by *T. versicolor*.

334

335 **3.3. Calculation of mass balances**

336 A ^{13}C -mass balance of labelled DCF and BP3 was performed across four different
337 sections over time i) ^{13}C remaining in the liquid media as non-transformed parent
338 compound, ii) ^{13}C newly formed byproducts in the media, iii) ^{13}C mineralized as carbon
339 dioxide, iv) ^{13}C incorporated into fungal biomass (Fig. 5). Estimation of byproducts was
340 calculated by subtracting to the initial amount of ^{13}C added in form of parent compound,
341 the remaining non-transformed parent compound, the amount accumulated into
342 biomass and mineralization. With regards to the ^{13}C calculated as incorporated into
343 fungal biomass, it is not possible to distinguish between the ^{13}C assimilated into
344 biomass and ^{13}C deriving from the accumulation of labelled parent compounds and/or
345 byproducts into the fungus cell. However, amino acid-SIP allows us to confirm that BP3
346 was used as carbon source whereas DCF degradation might proceed via
347 cometabolism or detoxification mechanisms. As observed in Fig. 5B, DCF could be
348 rapidly transformed to intermediates that would be slightly removed from the media
349 with a gradual accumulation into the fungal biomass. At the end of the incubation, ~
350 90% of DCF remained either as byproduct or accumulated into the cells. As observed
351 in Fig. 5A, mineralization of BP3 did not reach a plateau, suggesting that higher
352 mineralization rates could be reached if cultures were incubated longer. The mass
353 balance fits well with previous evidences of BP3 degradation by *T. versicolor*, since
354 30% of the initial BP3 was reported to be in the medium as glycoconjugate the ninth
355 day of incubation (Gago-Ferrero et al., 2012).

356

357 **3.4. Conclusions**

358 The use of amino acid-SIP and EA-IRMS techniques allowed us determining whether
359 the fungus used the tested emerging contaminants as carbon source for e.g. amino

360 acid biosynthesis or, on the contrary, the elimination process occurred via alternative
361 mechanisms. The use of these techniques are relevant for white-rot fungi due to the
362 complexity of the enzymatic system involved in the transformation of contaminants that
363 include i) cometabolism (ligninolytic enzymes, i.e. laccases and peroxidases), ii)
364 detoxification mechanism (i.e. cytochrome P450), and iii) metabolism (i.e. via lipid or
365 amino acid synthesis). By using amino acid-SIP, unequivocal use of xenobiotics in
366 metabolism can be proved, and it is more reliable than indirect evidences such as the
367 removal of the target compound when added as sole carbon source (Prenafeta-Boldú
368 et al., 2001), mineralization of xenobiotics by measuring isotopic signature of emitted
369 CO₂ (Tuomela et al., 1999), or disappearance of both parent compounds and
370 byproducts (Marco-Urrea et al., 2010). In all, the use of amino acid-SIP can shed light
371 on the fate of xenobiotics during white-rot fungi degradation and help to improve
372 bioremediation strategies using these organisms.

373

374 **Acknowledgements**

375 Authors would like to acknowledge Petra Bombach (UFZ) for her help in the
376 mathematical calculations behind the isotopic labelling and to Magdalena Grifoll (UB)
377 for their kindness on sharing their laboratory for some experimental settings. The work
378 was supported by the Spanish Ministry of Economy and Competitiveness (project ref
379 CTQ2010-21776-C02-01). The Department of Chemical Engineering of the Universitat
380 Autònoma de Barcelona is a member of the *Xarxa de Referència en Biotecnologia* of
381 *Generalitat de Catalunya*. Marina Badia was supported by a PIF predoctoral grant from
382 Universitat Autònoma de Barcelona.

383

384 **References**

385 Al-Rajab, A.J., Sabourin, L., Lapen, D.R., Topp, E., 2010. The non-steroidal anti-
386 inflammatory drug diclofenac is readily biodegradable in agricultural soils. The
387 Science of the total environment 409, 78–82.

388 Bastida, F., Rosell, M., Franchini, A.G., Seifert, J., Finsterbusch, S., Jehmlich, N.,
389 Jechalke, S., Bergen, M. Von, Richnow, H.H., 2010. Elucidating MTBE
390 degradation in a mixed consortium using a multidisciplinary approach. FEMS
391 Microbiology Ecology 73, 370–384.

392 Bastida, F., Jechalke, S., Bombach, P., Franchini, A.G., Seifert, J., Von Bergen, M.,
393 Vogt, C., Richnow, H.H., 2011. Assimilation of benzene carbon through multiple
394 trophic levels traced by different stable isotope probing methodologies. FEMS
395 Microbiology Ecology 77, 357–369.

396 Beaudette, L.A., Davies, S., Fedorak, P.M., Owen, P., Pickard, M.A., Beaudette,
397 L.E.E.A., Ward, O.P., 1998. Comparison of Gas Chromatography and
398 Mineralization Experiments for Measuring Loss of Selected Polychlorinated
399 Biphenyl Congeners in Cultures of White Rot Fungi. Applied and environmental
400 microbiology 64, 2020–2025.

401 Blázquez, P., Casas, N., Font, X., Gabarrell, X., Sarrà, M., Caminal, G., Vicent, T.,
402 2004. Mechanism of textile metal dye biotransformation by *Trametes versicolor*.
403 Water research 38, 2166–72.

404 Brausch, J.M., Rand, G.M., 2011. A review of personal care products in the aquatic
405 environment : Environmental concentrations and toxicity. Chemosphere 82, 1518–
406 1532.

407 Coplen, T.B., Brand, W.A., Gehre, M., Gröning, M., Meijer, H.A.J., Toman, B.,
408 Verkouteren, R.M., 2006. New Guidelines for $\delta^{13}\text{C}$ Measurements. Analytical
409 Chemistry 78, 2439–2441.

410 Duan, Y.-P., Meng, X.-Z., Wen, Z.-H., Ke, R.-H., Chen, L., 2013. Multi-phase
411 partitioning, ecological risk and fate of acidic pharmaceuticals in a wastewater
412 receiving river: the role of colloids. The Science of the total environment 447, 267–
413 73.

414 European Commission, 2002. Commission Directive 2002/72/EC of 6 August 2002
415 relating to plastic materials and articles intended to come into contact with
416 foodstuffs. Official Journal of the European Communities L220.

417 European Commission, 2007. Commission Staff Working Document on the
418 implementation for the “Community Strategy for Endocrine Disrupters”- a range of
419 substances suspected of interfering with the hormone systems of humans and
420 wildlife. SEC (2007) 1635.

421 European Commission, 2012. Report from the Commission to the European Parliament
422 and the Council on the outcome of the review of Annex X to Directive 2000/60/EC
423 of the European Parliament and of the Council on priority substances in the field of
424 water policy. COM (2011) 875 final.

425 European Parliament, 2000. Directive 2000/60/CE of the European Parliament and of
426 the Council of 23 October 2000 establishing a framework for Community action in
427 the field of water policy., Official Journal of the European Communities L 327.

428 Fent, K., Zenker, A., Rapp, M., 2010. Widespread occurrence of estrogenic UV-filters in
429 aquatic ecosystems in Switzerland. Environmental Pollution 158, 1817–1824.

430 Font, X., Caminal, G., Gabarrell, X., Romero, S., Vicent, M.T., 2003. Black liquor
431 detoxification by laccase of *Trametes versicolor* pellets. Chemical Technology
432 554, 548–554.

433 Gago-Ferrero, P., Badia-Fabregat, M., Olivares, A., Piña, B., Blánquez, P., Vicent,
434 Teresa, Caminal, Gloria, Díaz-Cruz, M.S., Barceló, Damià, 2012. Evaluation of
435 fungal- and photo-degradation as potential treatments for the removal of
436 sunscreens BP3 and BP1. The Science of the total environment 427-428, 355–63.

437 García-Galán, M.J., Rodríguez-Rodríguez, C.E., Vicent, Teresa, Caminal, Gloria, Díaz-
438 Cruz, M.S., Barceló, Damià, 2011. Biodegradation of sulfamethazine by *Trametes*
439 *versicolor*. Removal from sewage sludge and identification of intermediate
440 products by UPLC-QqTOF-MS. The Science of the total environment 409, 5505–
441 12.

442 Golan-Rozen, N., Chefetz, B., Ben-Ari, J., Geva, J., Hadar, Y., 2011. Transformation of
443 the recalcitrant pharmaceutical compound carbamazepine by *Pleurotus ostreatus*:
444 role of cytochrome P450 monooxygenase and manganese peroxidase.
445 Environmental science & technology 45, 6800–5.

446 Harms, H., Schlosser, D., Wick, L.Y., 2011. Untapped potential: exploiting fungi in
447 bioremediation of hazardous chemicals. Nature reviews. Microbiology 9, 177–92.

448 Hata, T., Kawai, S., Okamura, H., Nishida, T., 2010. Removal of diclofenac and
449 mefenamic acid by the white rot fungus *Phanerochaete sordida* YK-624 and
450 identification of their metabolites after fungal transformation. Biodegradation 21,
451 681-9.

452 Hernando, M.D., Mezcuca, M., Fernández-Alba, a R., Barceló, D, 2006. Environmental
453 risk assessment of pharmaceutical residues in wastewater effluents, surface
454 waters and sediments. *Talanta* 69, 334–42.

455 Jakobs-Schönwandt, D., Mathies, H., Abraham, W.-R., Pritzkow, W., Stephan, I., Noll,
456 M., 2010. Biodegradation of a biocide (Cu-N-cyclohexyldiazonium dioxide)
457 component of a wood preservative by a defined soil bacterial community. *Applied*
458 *and environmental microbiology* 76, 8076–83.

459 Jelic, A., Gros, M., Ginebreda, A., Cespedes-sa, R., Ventura, F., Petrovic, M., Barcelo,
460 D., 2011. Occurrence , partition and removal of pharmaceuticals in sewage water
461 and sludge during wastewater treatment. *Water research* 5, 1165–1176.

462 Kaal, E.E.J., De Jong, E., Field, J.A., 1993. Stimulation of Ligninolytic Peroxidase
463 Activity by Nitrogen Nutrients in the White Rot Fungus Stimulation of Ligninolytic
464 Peroxidase Activity by Nitrogen Nutrients in the White Rot Fungus *Bjerkandera sp.*
465 Strain BOS55. *Applied and environmental microbiology* 59, 4031–4036.

466 Liu, Y., Ying, G., Shareef, A., Kookana, R.S., 2011. Simultaneous determination of
467 benzotriazoles and ultraviolet filters in ground water , effluent and biosolid
468 samples using gas chromatography – tandem mass spectrometry. *Journal of*
469 *Chromatography A* 1218, 5328–5335.

470 Lu, H., Chandran, K., 2010. Diagnosis and quantification of glycerol assimilating
471 denitrifying bacteria in an integrated fixed-film activated sludge reactor via ¹³C
472 DNA stable-isotope probing. *Environmental science & technology* 44, 8943–9.

473 Marco-Urrea, E., Parella, T., Gabarrell, Xavier, Caminal, Gloria, Vicent, Teresa,
474 Adinarayana Reddy, C., 2008. Mechanistics of trichloroethylene mineralization by
475 the white-rot fungus *Trametes versicolor*. *Chemosphere* 70, 404–10.

476 Marco-Urrea, E., Pérez-Trujillo, M., Vicent, T., Caminal, G., 2009. Ability of white-rot
477 fungi to remove selected pharmaceuticals and identification of degradation
478 products of ibuprofen by *Trametes versicolor*. *Chemosphere* 74, 765–772.

479 Marco-Urrea, E., Pérez-Trujillo, M., Cruz-Morató, C., Caminal, G., Vicent, T., 2010.
480 Degradation of the drug sodium diclofenac by *Trametes versicolor* pellets and
481 identification of some intermediates by NMR. *Journal of Hazardous Materials* 176,
482 836–842.

483 Marco-Urrea, E., Seifert, J., Von Bergen, M., Adrian, L., 2012. Stable isotope peptide
484 mass spectrometry to decipher amino acid metabolism in *Dehalococcoides* strain
485 CBDB1. *Journal of bacteriology* 194, 4169–77.

486 Morasch, B., 2013. Occurrence and dynamics of micropollutants in a karst aquifer.
487 *Environmental pollution* 173, 133–7.

488 Murray, K.E., Thomas, S.M., Bodour, A.A., 2010. Prioritizing research for trace
489 pollutants and emerging contaminants in the freshwater environment.
490 *Environmental Pollution* 158, 3462–3471.

491 Prenafeta-Boldú, F.X., Luykx, D.M.A.M., Vervoort, J., de Bont, J.A.M., 2001. Fungal
492 metabolism of toluene: monitoring of fluorinated analogs by magnetic resonance
493 spectroscopy. *Applied Environmental Microbiology* 67, 1030-4.

494 Rodarte-Morales, A.I., Feijoo, G., Moreira, M.T., Lema, J.M., 2012. Biotransformation
495 of three pharmaceutical active compounds by the fungus *Phanerochaete*
496 *chrysosporium* in a fed batch stirred reactor under air and oxygen supply.
497 *Biodegradation* 23, 145-56.

498 Schreiner, K.M., Filley, T.R., Blanchette, R. a, Bowen, B.B., Bolskar, R.D., Hockaday,
499 W.C., Masiello, C. a, Raebiger, J.W., 2009. White-rot basidiomycete-mediated
500 decomposition of C60 fullerol. *Environmental science & technology* 43, 3162–8.

501 Tuomela, M., Lyytika, M., Oivanen, P., Hatakka, A., 1999. Mineralization and
502 conversion of pentachlorophenol (PCP) in soil inoculated with the white-rot fungus
503 *Trametes versicolor*. *Soil Biology and Biochemistry* 31, 65–74.

504 Wells, T., Ragauskas, A.J., 2012. Biotechnological opportunities with the β -ketoadipate
505 pathway. *Trends in biotechnology* 30, 627–37.

506 Yang, S., Hai, F.I., Nghiem, L.D., Price, W.E., Roddick, F., Moreira, M.T., Magram,
507 S.F., 2013. Understanding the factors controlling the removal of trace organic
508 contaminants by white-rot fungi and their lignin modifying enzymes: a critical
509 review. *Bioresource technology* 141, 97–108.

510

511

512 **Figure 1.** Time course degradation of DCF (A) and BP3 (B). Symbols: uninoculated
513 controls with ^{12}C -DCF/ ^{12}C -BP3 (●), heat-killed controls with ^{13}C -DCF (■), controls
514 containing sodium azide with ^{13}C -DCF/ ^{13}C -BP3 (▼), experimental cultures with ^{12}C -
515 DCF/ ^{12}C -BP3 (○) and experimental cultures with ^{13}C -DCF/ ^{13}C -BP3 (Δ).

516

517 **Figure 2.** A) Carbon dioxide produced every three days in cultures of *T. versicolor*
518 spiked with DCF. Symbols: controls containing sodium azide with ^{12}C -DCF (●) and ^{13}C -
519 DCF (○); experimental cultures with ^{12}C -DCF (▼) and ^{13}C -DCF (Δ). B) Cumulative
520 $^{13}\text{CO}_2$ production in cultures of *T. versicolor* spiked with either ^{13}C -BP3 (●) or ^{13}C -DCF
521 (○).

522

523 **Figure 3.** Carbon stable isotopic composition (atom%) of the fungal biomass spiked
524 with either DCF or BP3. Symbols: experimental cultures spiked with ^{12}C -BP3 (●), ^{12}C -
525 DCF (▼), ^{13}C -BP3 (○), and ^{13}C -DCF (Δ).

526

527 **Figure 4.** Carbon stable isotopic composition (atom%) of the amino acids in cultures
528 spiked with ^{12}C -BP3 and ^{13}C -BP3 at different experimental times. Values were
529 corrected for the carbon introduced during derivatization.

530

531 **Figure 5.** Mass balance of ^{13}C in BP3 (A) and DCF (B) experiments. In black non-
532 transformed ^{13}C -BP3/ ^{13}C -DCF remaining in the media, in dark grey estimated ^{13}C
533 remaining in the media in form of byproducts to complete the mass balance, in light
534 grey ^{13}C into fungal biomass, and in white ^{13}C mineralized ($^{13}\text{CO}_2$).

535